Sensors & Transducers, Vol. 189, Issue 6, June 2015, pp. 128-136

www.sensorsportal.com

Sensors & Transducers

http://www.sensorsportal.com

An Improved Analytical Approach for Estimation of Misalignment Error of Sensing Axis in MEMS Accelerometers using Simple Tilt Measurements

R. K. Bhan, Shaveta, Imran, Ramjai Pal and Shankar Dutta
Solid State Physics Laboratory, DRDO, Lucknow Road, Timarpur, Delhi, India – 110054
Tel.: 91-011-23903403
E-mail: bhan@sspl.drdo.in

Received: 15 May 2015 /Accepted: 15 June 2015 /Published: 30 June 2015

Abstract: A simple experimental method and improved analytical approach based on tilt measurements (output versus angle) is presented to determine the misalignment error in sensing axis direction of single, two or three-axis accelerometer sensors. The approach is advantageous in resolving and measuring the error because the accuracy is enhanced by using identification that is based on differential and reciprocal differential data of the tilt measurements. Furthermore, the method does not require three accelerometers and there is no need for determination of matrix coefficients as is the practice presently followed in the literature. The method is validated on actual prototype sensors fabricated in our laboratory. The experimental results agree well with the theoretical predictions. The estimates obtained from the proposed method compares well with conventional analytical fit method that requires prior knowledge of sensitivity parameter. *Copyright © 2015 IFSA Publishing, S. L.*

Keywords: Accelerometer, MEMS sensors, IMU, Misalignment, Calibration, Sensing axis.

1. Introduction

MEMS based accelerometers are widely used in automotive, consumer and industrial markets. They have replaced established, expensive and high end fragile electromechanical devices. Further they offer same or better performance at lower cost, lower power consumption, smaller size and greater strength. They have already penetrated defense programs including navigation control. The major advantage of MEMS sensors being their reliability, accuracy and excellent price performance. Particularly for defense inertial navigational applications, they are preferred because of low cost due to batch process, rugged assembly, low weight and size and important of all because of their ability to satisfy high bias stability performance.

There are many applications where these sensors (three for 3 axes) are used for attitude measurements (e.g., aircraft, satellites, UAVs, and underwater vehicles). The literature is rich with calibration solutions for determining the null shifts, scale factor errors, and cross coupling [1-2]. Most of these methods are based on static calibration in which we determine the matrix coefficients and zero bias of a linear modeled accelerometer. Conventionally, rotary table is used to calibrate an accelerometer. However a precision rotary table is usually expensive and the process is time-consuming [3, 4]. A lot of workers in the field suggested approaches which are mainly focussing on complete calibration of IMU that use three/tri-axial accelerometers and gyroscopes besides requiring solution of complex matametical equations or algorithims. For example, the method suggested by

Tee etal [5] require solution of mathematical equations for identification of singularity by principal of matrix rank. Lötters [6] et al suggested procedure for in-use calibration of tri-axial accelerometers that uses the fact that the modulus of the acceleration vector measured with a tri-axial accelerometer equals 1g under quasi-static conditions. WT Fong [7] et al presented methods for tri-axial accelerometers setups in a MEMS based inertial measurement unit (IMU) that depend on the Earth's gravity as a stable physical calibration standard. H Zhang et al [8] proposed improved multi-position calibration for IMUs that uses outputs of gyroscopes and accelerometers. Syed *et al* [9] proposed a new multi-position (compared to traditional calibration methods, e.g. six-position and rate test calibration) method that does not require special aligned mounting and has been adapted to compensate for the primary sensor errors. *Isaac* and *Peter* [10] proposed a method for accelerometer and gyro that requires a rate table but does not require a mechanical platform for calibration and developed improved algorithm for low cost function for calibration. Nieminen *et al* [11] proposed an enhanced multi-position calibration method using a rate table that is enhanced to exploit also the centripetal accelerations caused by the rotation of the table resulting in significantly enhanced accuracy at the cost additional numerical calculations. Kim and Golnaraghi [12] presented a reliable calibration procedure of an inertial measurement unit using an optical position tracking system. Won, S.-h.P and Golnaraghi [13] presented a new triaxial accelerometer calibration method using a mathematical model of six calibration parameters that is applicable in extreme cases of high (1000 $V/(m/s^2)$) and low (0.001 $V/(m/s^2)$) gain factors. Panahandeh et al [14] proposed a method for calibration of accelerometer cluster of an IMU that does not rely on using a mechanical calibration platform that rotates the IMU into different precisely controlled orientations using the maximum likelihood estimation method. The accuracy of the proposed calibration method was compared with the Cramer- ´ Rao bound for the considered calibration problem.

Using all the above said methods are suited for complete IMU development and the cost of a mechanical platform and rate table can many times exceed the cost of developing a MEMS sensor based IMU besides requiring solution of complex mathematical equations/algorithms.

Non-parallelisms in various sub components of accelerometers due to imperfect fabrication or machining processes are practical realities. These non-idealities yield to misalignment of sensing axis and hence needs to be controlled and characterized. It is generally true that the sensor suite is never perfectly aligned with the body axis including accelerometers mounted on packages which are in turn are mounted on matching sockets. These sockets are further mounted on evaluation PCB boards. Because of several planes or the joints sensors are misaligned due to imperfect fabrication or machining processes. All these non-idealities lead to misalignment of sensing axis. For simple initial laboratory characterization of a single axis accelerometer, we propose a simple low cost laboratory solution for measurement of misalignment error of sensing axis based on use of low cost inclinometers. The accuracy of the method is improved by analyzing the data in differential mode which enhances the slope changes compared to rate table tests.

In this paper, we present a new analytical approach based on differential and reciprocal differential of data of tilt measurement for determining the axis misalignment error i.e. the extent to which the accelerometers true sensitive axis deviates from being perfectly orthogonal to the accelerometers reference mounting surface when mounted to flat surface. Majority of manufacturers term this specification as "input axis misalignment".

Section 2 presents the theoretical basis, Section 3 describes the experimental details, Section 4 discusses the results and finally Section 5 briefly summarizes the conclusions.

2. Theoretical

It is assumed that the accelerometer is a single axis and has the sensing axis along z-direction as shown in Fig. 1. The scale factors, misalignment angles and zero bias are assumed to be invariant to time. As shown in this figure if the sensor is mounted horizontally such that its sensing axis is facing vertically (Fig. 1 top right) upwards then the sensor will be under 1g or it face -1g if flipped upside down. However, if the sensor is tilted by 90^0 angle, then it faces 0g acceleration (Fig. 1 top center). Further it will face intermediate value between 1g and 0 g if tilted by an angle θ as shown in this figure (Fig. 1 top right). The output is expected to follow the sine-wave as a function of angle θ (Fig. 1 bottom).

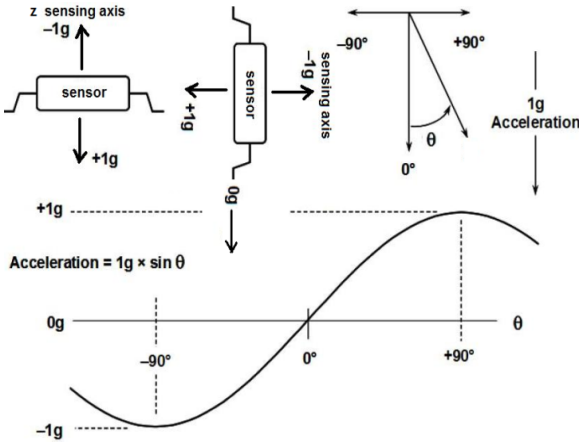

Fig. 1. The ideal output of accelerometer as a function of tilt angle θ following a sinewave.

$$V=A+B\times Sin(\theta)\times g, \quad (1)$$

where V is the output in mV, A is the offset zero bias offset in Volts and B is the sensitivity in Volts/g.

The problem however is that as mentioned above, there always will be some mounting error, which results in non-idealities in this measurement. Let the total mounting angle misalignment or input axis misalignment error be Err then the output is expected to follow:

$$V=A+B\times Sin(\theta+Err)\times g \quad (2)$$

Fig. 2 shows the ideal plot of this eqn. where A=2 Volts and Err=0^0 and sensitivity B is 0.1 V/g with a variation of ±10 mV. In addition it also shows a plot for a small sensitivity of 0.025 V/g. It can be seen from this figure that output follows a sine wave and hence shows the expected peaks at ± 90^0 of angle. It is argued here that this peak can be utilized to estimate the misalignment error Err. Fig 3a show the effect of misalignment error on peak position. Fig 3b shows the magnified view of Fig. 2 near the peak position at -90^0. It may be seen that one can clearly determine the horizontal shift of peak position e.g. -5^0 and 2^0 in this figure. The shift in position of this peak from -90^0 (or from +90^0) is a measure of misalignment error. If the peak is sharp, then the identification of the peak is relatively easy. However, it may be seen from Fig. 2 that as the sensitivity decreases e.g. B=0.025 mV/g, this peak becomes shallow and its identification becomes difficult because the FWHM of this peak increases to 138^0 from 117^0 when S=0.1V/g. For accurate determination it is desirable to have very small FWHM. The problem becomes pronounced particularly for accelerometers having a high g e.g. 100 g or more because sensitivity is inversely proportional to g. For example, commercial MEMS accelerometer of Colibrys has sensitivity of 10 mV/g for 200 g compared to 2000 mV/g for 1g range [15].

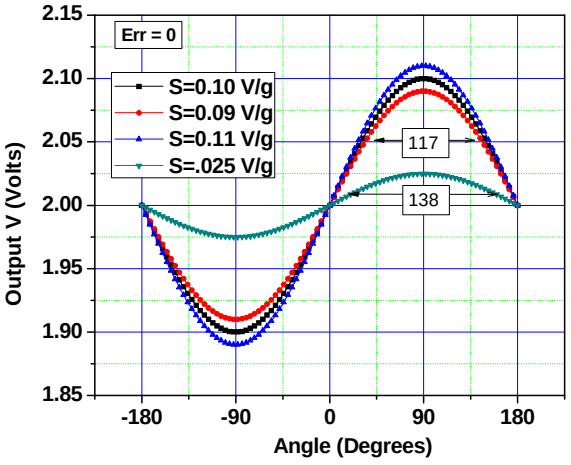

Fig. 2. The ideal theoretical output of accelerometer as a function of θ for various values of sensitivity. It is assumed that misalignment error is zero in this case.

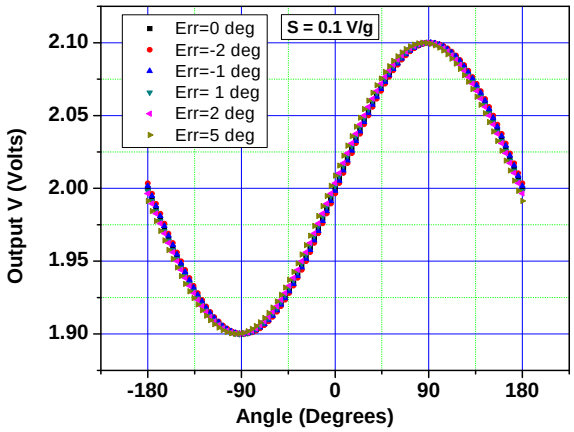

Fig. 3a. The ideal theoretical output of accelerometer as a function of θ for various values of tilt angles. It is assumed that sensitivity is constant in this case.

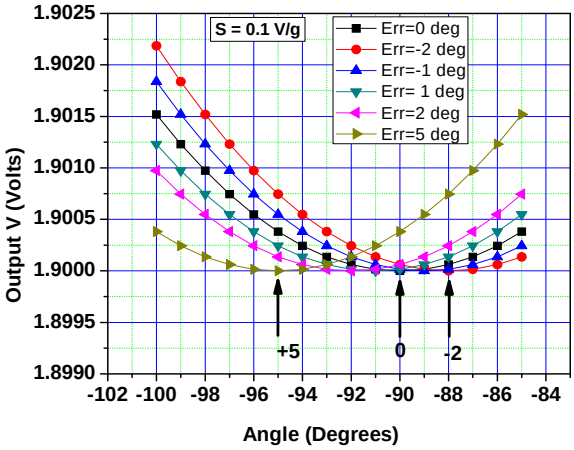

Fig. 3b. The magnified view of Fig. 3a showing the shifted position of minimas at +5^0, -2^0 along with 0^0 position.

To enhance the detection of shallow peaks, it is proposed in this paper that one can exploit the data of peak position itself. Since at the peak position we have a maxima/minima and mathematically at this point we know that dV/dθ =0. Therefore, it is argued that one should take the differential of the data and locate the zero cross over point in the Y-axis. This X-coordinate of this cross over point will yield the misalignment error directly with improved accuracy because here we are working with differential of the data. Fig. 4a and 4b shows the theoretical plot of V vs. θ and corresponding dV/dθ vs. θ with misalignment of 0^0 and 5^0. One can clearly see from Fig. 4b that dV/dθ crosses the zero value at 5^0 away from +90^0 or -90^0. Hence the zero cross over point of dV/dθ determines the misalignment error. The ultimate resolution will be limited by the small interval of angular step that is used in taking the data. This concept will be later tested on actual experimental data in Section 4.

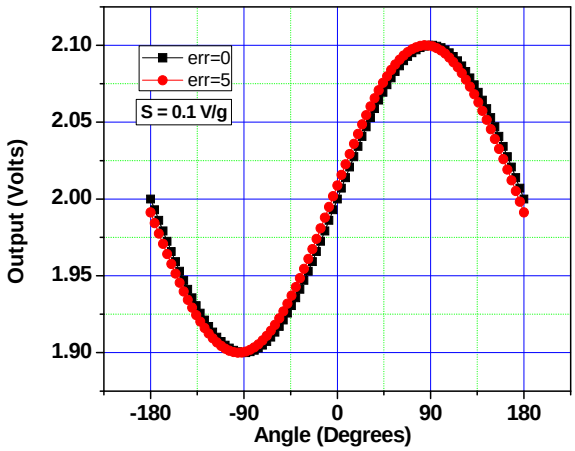

Fig. 4a. The ideal theoretical output of accelerometer as a function of θ for two values of tilt angles viz. 0^0 and 5^0. It is assumed that sensitivity is constant in this case.

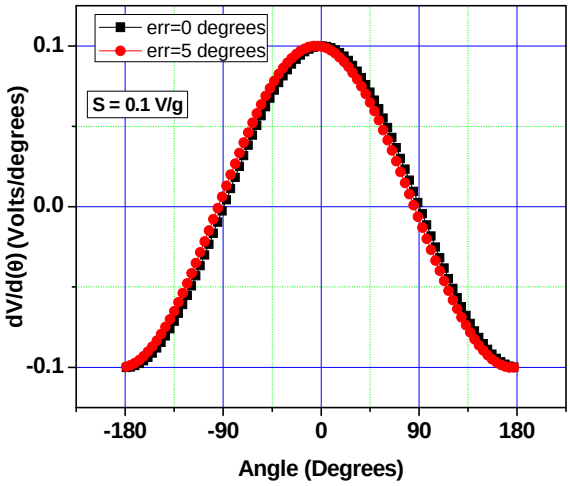

Fig. 4b. The graph of differential of output of accelerometer as a function of θ for two values of misalignment viz. 0^0 and 5^0. It is assumed that sensitivity is constant in this case.

For situations where the experimental data is corrupted by the noise and the accurate location of zero cross over point is difficult, we propose to use another derived parameter called reciprocal differential i.e. $(dV/d\theta)^{-1}$. Mathematically, there are vertical asymptotes at $\pi/2$ intervals in this function and the detection of such asymptotes are generally vivid in experimental data as will be shown here later. Midway intersection of asymptotes on the X-axis is taken as the misalignment error. Figs. 5a and 5b show such plots when error is 0^0 and 5^0. Clearly the plots show 5^0 shifts from -90^0 or $+90^0$.

The added advantage of using proposed differential or reciprocal differential of the data is that one can improve the basic detection limit by extrapolating the data between the points where slope crosses sign from +ve to -ve or vice-versa. This will be shown later using actual experimental data.

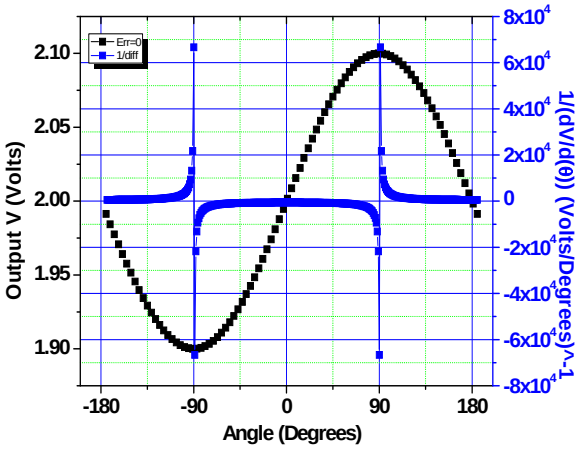

Fig. 5a. The graph of reciprocal differential of output of accelerometer as a function of θ for 0^0 misalignment error. It is assumed that sensitivity is constant in this case.

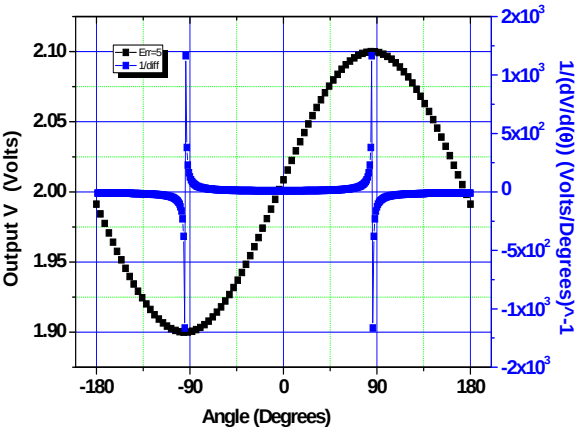

Fig. 5b. The graph of reciprocal differential of output of accelerometer as a function of θ for 5^0 misalignment error. It is assumed that sensitivity is constant in this case.

3. Experimental

The crab type capacitive microaccelerometer structures were realized using a three mask dissolved wafer process (DWP). The structure consists of boron doped silicon inertial proof–mass suspended over a glass pit that was created in 7740 Pyrex glass substrate using wet etching. A bottom plate capacitor contact was made of Ti plus Gold. The depth of cavity is about 5-8 microns. Further, in the Silicon wafer deep boron diffusion was carried out at 1175 ºC to achieve boron doping ~ 1×10^{20} atoms/cc over a depth of about 10-12 µm. This heavily boron doping will act as etch stop layer during the final stages of DWP process in chemical etchant. Brief details of the fabrication steps of the Microccelerometer structure are shown in Fig. 6(a), SEM picture of final fabricated device is shown in Fig. 6b and final prototype is shown in Fig. 6c.

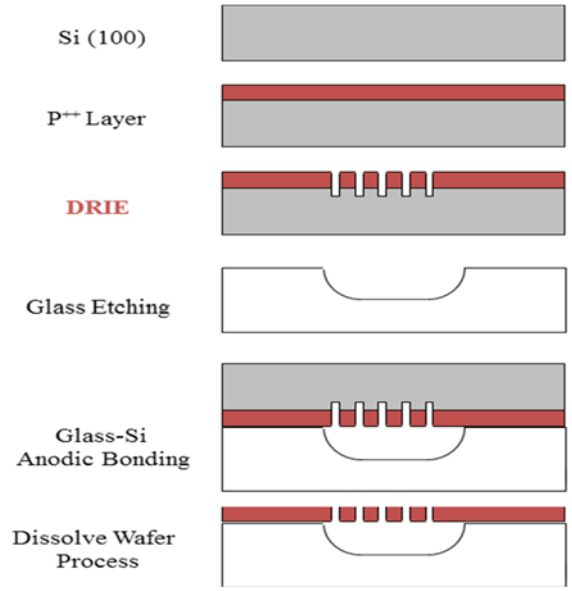

Fig. 6a. Brief fabrication steps showing Si <100> wafer followed by p^{++} boron diffusion, DRIE of Crab Type, Glass cavity etching, Glass–Si anodic bonding and finally Dissolve Wafer Process (DWP) for release of structure.

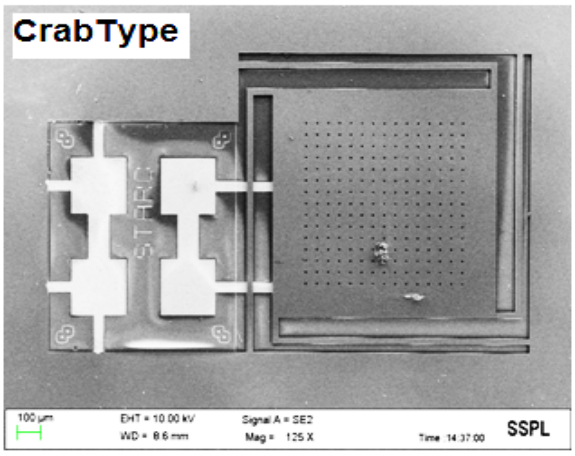

Fig. 6b. SEM pictures of crab type accelerometer structure.

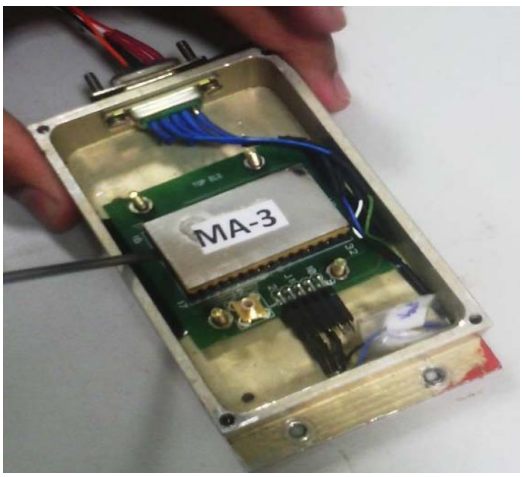

Fig. 6c. A photograph of prototype along with a shielding box of crab type accelerometer structure.

Interface circuit for converting the variation in capacitance into voltage is implemented using a standard off the shelf ASIC, MS3110 from Irvine Sensors. MS3110 is a general purpose, ultra noise CMOS IC that requires only a single +5 V DC supply and some decoupling components. The ASIC is capable of sensing capacitance changes down to 4aF/√Hz. It can interface with either a differential capacitor pair or a single capacitive sensor [16].

Further detailed behavior of accelerometer analog output voltage as a function of inclination angle θ was measured from -90^0 to $+90^0$ with an inclinometer from Boch & Lamb (model no. DWM 40L) having a resolution of 0.1^0 (Fig. 7). It displays the value of angle digitally. The measurements near -90^0 were extended up to -110^0 so that the minima are located. Before starting the measurement, the platform was adjusted horizontally using an electronic spirit level (resolution, 0.1^0). It may be stressed here that the ultimate possible measurement resolution will be limited by the resolution of the equipment with which horizontal alignment of the table is done and finally by the resolution of the inclinometer used for taking V vs. θ measurement which again was 0.1^0 in our case. The results will be shown in next section.

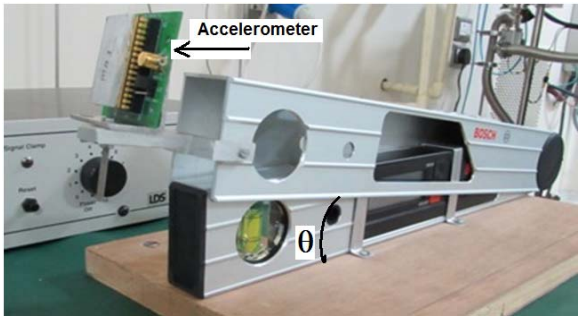

Fig. 7. Tilt measurement set up showing an inclinometer (Bosch make) in which accelerometer along with its evaluation board is mounted at its front end. The meter has a digital display of angle with resolution of 0.1^0.

4. Results and Discussions

About ten prototype micro accelerometers of the type as shown in Fig. 6c and with a sensitivity of 100 mV/g were prepared. Out of these, three pieces having different zero bias offset and other characteristics were selected for further investigation. Selection of such three pieces (having appreciable variation in characteristics) was motivated by the fact that we want to check the applicability of our proposed method over a large range. Fig. 8 shows the V vs. θ plots for three sensors MA6, MA7 and MA8. It may be seen from this figure that corresponding zero bias offset is 2.09, 2.15 and 2.25 Volts respectively. Further, the measurement was taken beyond -90^0 to locate the minima that will be utilized to estimate the misalignment error.

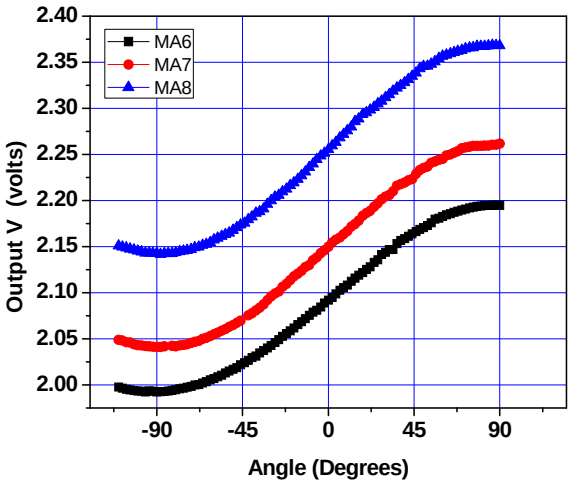

Fig. 8. The output of three prototype accelerometers as a function of θ.

Next, using the above mentioned zero bias offset values analytical fit to equation 2 was obtained wherein the measured value of B viz. 100 mV/g (from +/- 1g flip test) was used. The results are shown in Figs. 9a to 9c. This is method used by many workers in the field. The difficulty with this method is that it requires accurate knowledge of sensitivity from independent measurement. Otherwise it will not be unique fit because two parameters viz. B and Err are unknown. The values of misalignment error obtained by this method for MA6, MA7 and MA8 are 0.57^0, 0.56^0 and 0.50^0 respectively. As stated earlier in section 3, our estimation is accurate to within 0.1^0 only. One can further improve upon these numbers by using inclinometer with improved resolution or even rate table which generally has better resolution.

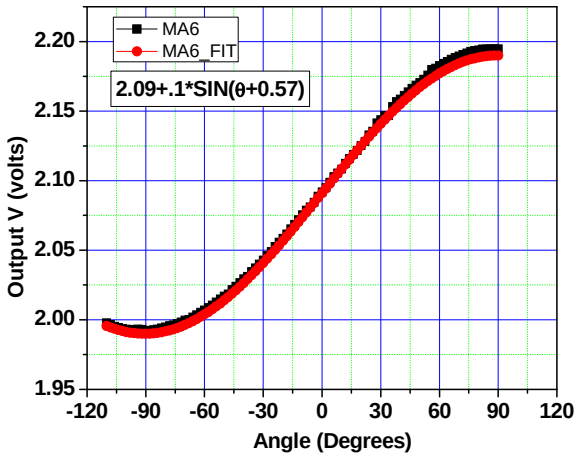

Fig. 9a. The output of MA6 accelerometer along with its analytical fit to equation 2.

As stated in Sections 1 and 2, we propose to exploit the minima and use the differential of the data for estimation of the misalignment parameter Err. Figs. 10a to 10c show the measured data along with the differential data i.e. dV/dθ vs. θ.

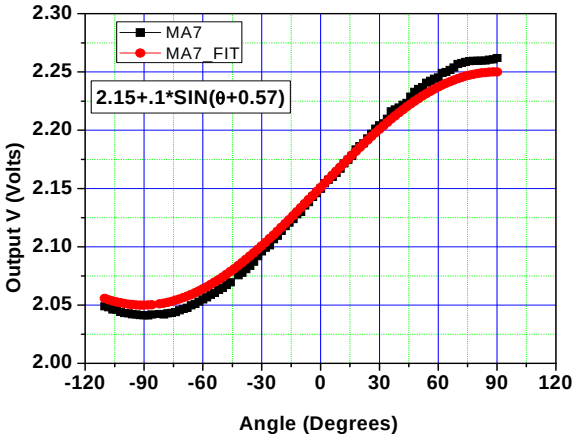

Fig. 9b. The output of MA7 accelerometer along with its analytical fit to equation 2.

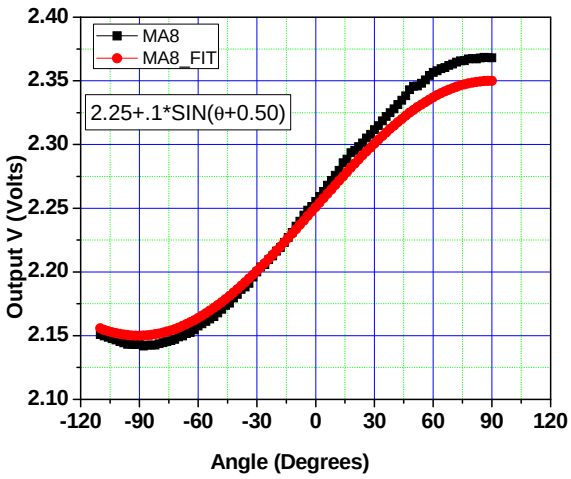

Fig. 9c. The output of MA8 accelerometer along with its analytical fit to equation 2.

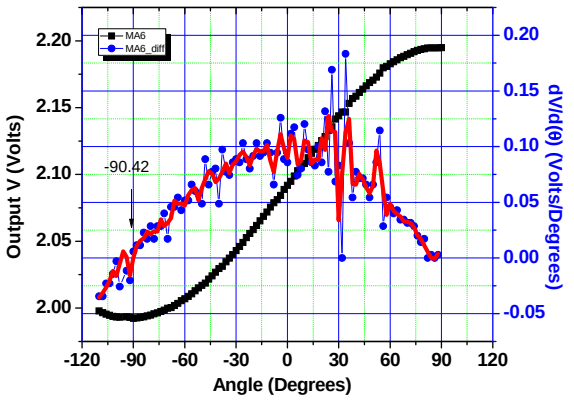

Fig. 10a. The graph of differential and actual of output of accelerometer MA6 as a function of θ. The data of differential output has further been fitted to smoothened data.

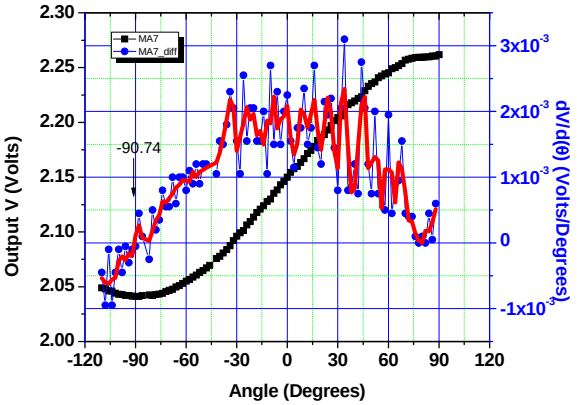

Fig. 10b. The graph of differential and actual of output of accelerometer MA7 as a function of θ. The data of differential output has further been fitted to smoothened data.

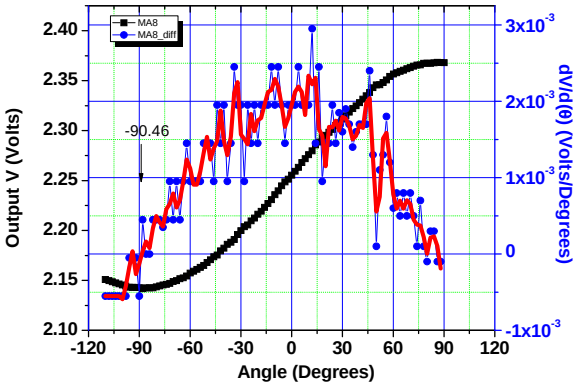

Fig. 10c. The graph of differential and actual of output of accelerometer MA8 as a function of θ. The data of differential output has further been fitted to smoothened data.

As expected, the differential of the basic data (a sine function) follows cosine function. It may be seen from these figs. that the added advantage of using differential data clearly shows the noise in original data. We have used smoothening algorithm of software Origin 8.0 for improving the quality of data. The smoothened curve has been overlapped on the differential curve. Next the zero cross over point is located in these figures that will be used for determining the Err parameters. The values obtained for MA6, MA7 and MA8 are -90.42^0, -90.86^0 and -90.46^0 respectively. Deviation of these values from -90^0 represents the Err. The absolute magnitudes of these three values in our case are 0.42^0, 0.74^0 and 0.46^0 respectively. The added advantage of using the differential data instead of original data i.e. $dV/d\theta$ vs. θ is that there will be typically three positions on this curve at -90^0 , 0^0 and $+90^0$ where this deviation can be measured and all of them are expected to yield same information i.e. misalignment error. Depending upon the noise in the measured data, one can choose the best position. For example it may be seen from our measured data from Figs. 10a to 10c, -90^0 is the position having least noise. Using this measure, we estimate the absolute value of Err parameter for MA6, MA7 and MA8 as 0.42^0, 0.74^0 and 0.46^0 respectively. These values agree reasonably well with estimates from analytical fit.

Further, as discussed in Section 2, for situations where the experimental data is corrupted by the noise and the accurate location of zero cross over point is spread over large range, we propose to use another derived parameter called reciprocal differential i.e. $(dV/d\theta)^{-1}$. The advantages of working with $(dV/d\theta)^{-1}$ vs. θ were already discussed in Section 2. Figs. 11a to 11c show these plots for MA6, MA7 and MA8. Procedure for obtaining the parameter Err is same as was discussed in Section 2. Using those procedures, we estimate the absolute value of Err parameter for MA6, MA7 and MA8 as 1^0, 1^0 and 1^0 respectively. Basically, the asymptotes shown in Figs. 11a to 11c should be used to identify the peaks quickly. It may be seen from these values that disagreement between the estimate of Err parameter obtained from analytical fit and differential method is ±13.1 %, ±16.0 %, and ±4.0 % for MA6, MA7 and MA8. Table 1 summarizes the results.

Table 1a. Summary of estimated parameters using differential.

Device No.	Analytical FitErr (AErr)	Diff @ -90	Abs(Err) w.r.t. Diff	Disagree -ment %
	Degrees	Degrees	Degrees	
MA6	0.57	-90.42	0.42	±13.1 %
MA7	0.56	-90.74	0.74	±16.0 %,
MA8	0.50	-90.46	0.46	±4.0 %

Table 1b. Summary of estimated parameters using reciprocal differential.

Device No.	1/Diff +ve peak	1/Diff -ve peak	Avg of +ve & -ve peak	Abs(Err)
	Degrees	Degrees	Degrees	Degrees
MA6	-90.00	-92.00	-91.00	1.00
MA7	-88.00	-90.00	-89.00	1.00
MA8	-88.00	-90.00	-89.00	1.00

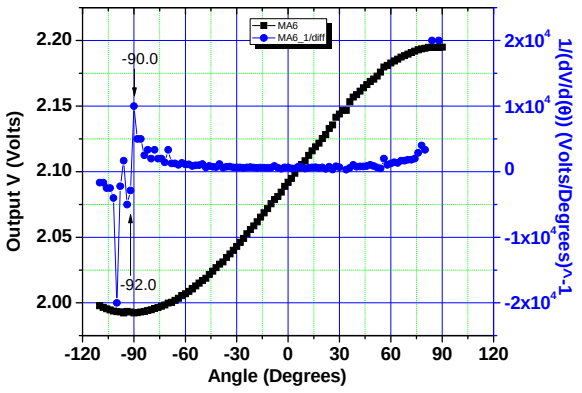

Fig. 11a. The graph of reciprocal differential and actual of output of accelerometer MA6 as a function of θ.

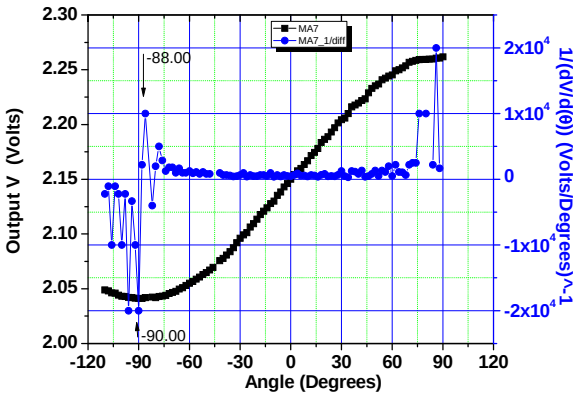

Fig. 11b. The graph of reciprocal differential and actual of output of accelerometer MA7 as a function of θ.

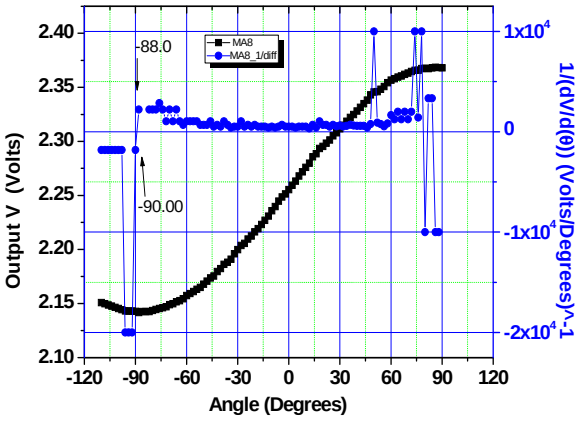

Fig. 11c. The graph of reciprocal differential and actual of output of accelerometer MA8 as a function of θ.

Finally, we tried to compare these values to the estimate obtained from known misalignments of various layers/sub-components which contribute to prototypes fabrication. The known non-parallelism in various sub components/layers of accelerometers due to imperfect fabrication or machining processes is given in Table 2.

Assuming all the misalignments add up in one direction only (Fig. 12) we can estimate the maximum possible misalignment error by using a simple formula (tanθ=Diff/Length using Table 2). The total misalignment by this estimate is 0.7085^0. However, in practice it is unlikely that all the layers will be misaligned in one direction only. Random misalignments are expected among the layers.

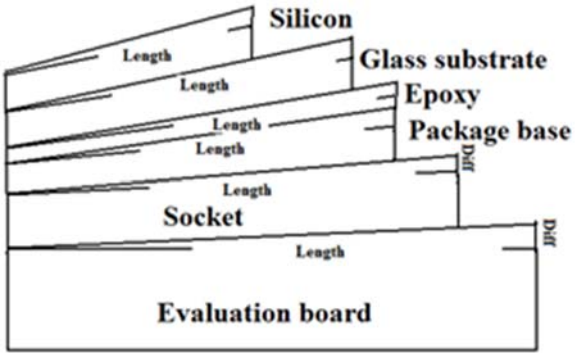

Fig. 12. The schematic of various sub components used in the assembly of prototype fabrication. Non-parallelisms in various sub components of accelerometers due to imperfect fabrication or machining processes have been depicted assuming gradients in all layers are pointing in one direction.

Table 2. Non-parallelisms in various sub components of accelerometers due to imperfect fabrication or machining processes.

Item	Shape	Dimensions	Thickness (min)	Thickness (max)	Diff (um)	Angle (Degrees)	
		Length (um)	Width (um)	microns	microns	microns	Degrees
Evaluation Board	Rectangle	50200	50200	1575	1725	150.0000	0.1712
Socket	Rectangle	40132	22733	5400	5600	200.0000	0.2855
Package base	Rectangle	40132	22733	940	1092	152.0000	0.2170
Epoxy	Rectangle	40000	22000	45	55	10.0000	0.0143
Glass substrate	Rectangle	8400	6825	699	701	2.0000	0.0136
Silicon	Rectangle	8400	6825	11	12	1.0000	0.0068
Maximum Total							**0.7085**

For example, in our case, the variations in manufacturing thickness variations of surfaces of socket are contributing maximum to misalignments viz. 0.2855^0. If the direction of the gradient is in opposite direction i.e. -0.2855^0, the total error reduces to 0.1374^0 assuming all other components are positive. Similarly assuming evaluation board contributes -0.1712^0 and all other layers are contributing in positive direction, the total error reduces to 0.3660^0. Any misalignment in opposite direction will always reduce the total error. It will be safe to assume that mean of two limits (least contributor and maximum contributor) will be the number most likely. This in our case is 0.4161^0

(socket and Silicon). This number compares well with the estimates of two out of three accelerometers i.e. MA6 and MA8. The point we want to stress is that estimates obtained by differential method agree reasonably well with indirect estimates obtained from Table 2. The trend of above results was repeatable on 4 set of other devices fabricated and measured in our laboratory.

In short we have demonstrated that one can measure the misalignment error in sensing axis of accelerometer by using a differential ($dV/d\theta$ vs. θ) and reciprocal differential ($(dV/d\theta)^{-1}$ vs. θ) data of basic V vs. θ plot. The proposed method has many advantages and estimates from this method compare well with analytical and other indirect methods.

5. Conclusions

In brief, using the tilt measurement data, a new analytical approach based on differential and reciprocal differential of data is proposed which does not require prior knowledge of other parameters. The method is applicable to single, two or three-axis sensors. The estimates from this method compare well with conventional analytical fit method and indirect estimates obtained from sub-componets. The method utilizes the position of minima form the data of tilt measurements wherein the derivative is zero and reciprocal derivative that shows an asymptote at the angle matching with the value misalignment error. The method is validated on actual prototype sensors fabricated in our laboratory.

Acknowledgement

The authors would like to thank Director, Solid State Physics Laboratory for his continuous support and for the permission to publish this work. Help from other colleagues of MEMS division are also acknowledged.

References

[1]. G. H. Elkaim and C. Foster, Extension of a non-linear, two-step calibration methodology to include non-orthogonal sensor axes, *IEEE Transactions on Aerospace Electronic Systems,* 44, 3, 2008, pp. 1070 - 1078.

[2]. J. Vasconcelos, G. H. Elkaim, C. Silvestre, P. Oliveira, and B. Cardeira, Geometric Approach to Strapdown Magnetometer Calibration in Sensor Frame, *IEEE Transactions on Aerospace Electronic Systems,* 47, 2, 2011, pp 1293 - 1306.

[3]. W. T. Fong, S. K. Ong, and A. Y. C. Nee, Methods for in-field user calibration of an inertial measurement unit without external equipment, *Measurement Science and Technology,* Vol. 19, 2008, pp. 1-11.

[4]. F. Ferraris, U. Grimaldi, and M. Parvis, Procedure for Effortless In-Field Calibration of Three-Axis Rate Gyros and Accelerometers, *Sensors and Materials,* Vol. 7, 1995, pp. 311-330.

[5]. Kian Sek Tee, Mohammed Awad, Abbas Dehghani, David Moser, Saeed Zahedi, Triaxial Accelerometer Static Calibration, in *Proceedings of the World Congress on Engineering WCE'11*, London, U. K., Vol. I, July 6 - 8, 2011, p. 1309.

[6]. J. C. Lötters, J. Schippe, P. H. Veltink, W. Olthuis, and P. Bergveld, Procedure for in-use calibration of triaxial accelerometers in medical applications, *Sensors and Actuators A: Physical,* Vol. 68, 1998, pp. 221-228.

[7]. W. T. Fong, S. K. Ong, and A. Y. C. Nee, Methods for in-field user calibration of an inertial measurement unit without external equipment, *Measurement Science and Technology,* Vol. 19, 2008, pp. 1-11.

[8]. Hongliang Zhang, Yuanxin Wu, Wenqi Wu, Meiping Wu and Xiaoping Hu, Improved multi-position calibration for inertial measurement units, *Measurement Science and Technology,* Vol. 21, No. 1, 2010, 015107.

[9]. Z. F. Syed, P. Aggarwal, C. Goodall, X. Niu and N. El-Sheimy, A new multi-position calibration method for MEMS inertial navigation systems, *Meas. Sci. Technol.,* 18, 2007, 1897.

[10]. Isaac Skog and Peter H¨andel, Calibration of a MEMS inertial measurement unit, in *Proceedings of the XVII IMEKO World Congress, Metrology for a Sustainable Development*, September, 17–22, 2006 Rio de Janeiro, Brazil.

[11]. Tuukka Nieminen, Jari Kangas, Saku Suuriniemi and Lauri Kettunen, An enhanced multi-position calibration method for consumer-grade inertial measurement units applied and tested, *Meas. Sci. Technol.,* Vol. 21, No. 10, 2010, 105204.

[12]. Kim, A. and Golnaraghi, M. F., Initial calibration of an inertial measurement unit using an optical position tracking system, in *Proceedings of the Position Location and Navigation Symposium (PLANS'04),* 26-29 April 2004, pp. 96 – 101.

[13]. Won, S.-H. P. and Golnaraghi, F., A Triaxial Accelerometer Calibration Method Using a Mathematical Model, *IEEE Transactions on Instrumentation and Measurement,* Vol. 59, No. 8, 2009, pp. 2144-2153.

[14]. G. Panahandeh, I. Skog, and M. Jansson, Calibration of the Accelerometer Triad of an Inertial Measurement Unit, Maximum Likelihood Estimation and Cramer-Rao Bound, in *Proceedings of the International Conference on Indoor Positioning and Indoor Navigation (IPIN),* 15-17 September 2010, Zurich, Switzerland.

[15]. http://www.colibrys.com/

[16]. Operation manual of MS3110 Universal Capacitive Readout IC, *Irvine Sensors Corporation*.